

Gum Arabic-Assisted TiO₂ Photoanode Fabrication for Dye-Sensitized Solar Cells Sensitized with Natural Dye Extracted from Bicolor Sorghum

Isa M Mukhtar¹, Aliyu K Isiyaku^{2,3}, Nicodemus Kure², Auwal M Imam^{4,5}, Isah Mustapha^{2,3}, Tasiu Jamila², and Ibrahim Mustapha⁶

¹ Department of State Industrial Extension Services, Raw Materials Research and Development Council, No. 17 Aguiyi Ironsi Street, Maitama District, FCT Abuja, Nigeria

² Department of Physics, Faculty of Physical Sciences, Kaduna State University, P.M.B. 2339, Kaduna, Kaduna State, Nigeria

³ Centre for Energy and Environmental Strategy Research, Faculty of Physical Sciences, Kaduna State University, P.M.B 2339, Kaduna, Kaduna State, Nigeria

⁴ Physics with Electronics Department, Airforce Institute of Technology (AFIT), Kaduna, Kaduna State, Nigeria

⁵ Nigeria Institute of Leather and Science Technology (NILEST), Zaria, Kaduna State, Nigeria.

⁶ Department of Physical and Life Sciences, National Air Space Research and Development Agency, Obasanjo Space Center, Lugbe FCT, Abuja, Nigeria

Corresponding E-mail: isamukhtar.m@rmrdc.gov.ng

Received 03-04-2026

Accepted for publication 12-06-2026

Published 25-06-2026

Abstract

The stability and efficiency of dye-sensitized solar cells (DSSCs) are often limited by the degradation of key components, including dyes, electrolytes, and electrodes. This study investigates the effect of gum Arabic as a biopolymeric binder on TiO₂ photoanode fabrication and the photovoltaic performance of DSSCs sensitized with a natural dye extracted from Sorghum bicolor grains. TiO₂ films were prepared using the doctor-blade technique with gum Arabic concentrations of 0.56 g (Sample A) and 1.25 g (Sample B). Fourier transform infrared (FTIR) spectroscopy revealed O–H and C–O–C functional groups that promote dye adsorption and film stability, while UV–Visible spectroscopy confirmed strong absorption in the ultraviolet–visible region, extending the spectral response of TiO₂. Photovoltaic performance was evaluated using current–voltage (I–V) measurements under dark and illuminated conditions. Sample B exhibited the best performance under illumination, with $V_{oc} = 0.60$ V, $J_{sc} = 1.50$ mA/cm², $V_{max} = 0.46$ V, $I_{max} = 1.15$ mA, $P_{max} = 5.3 \times 10^{-4}$ W, $FF = 0.59$, and $\eta = 0.53\%$. The improved performance is attributed to enhanced visible-light absorption by anthocyanin dye molecules, reduced charge recombination, and improved electron transport. These findings demonstrate the potential of gum Arabic-modified TiO₂ photoanodes and sorghum-derived natural dyes as low-cost and environmentally sustainable materials for DSSC applications.

Keywords: Dye-Sensitized Solar Cells (DSSCs); Sorghum bicolor; Gum Arabic; TiO₂ Photoanode; Natural Dye Sensitizers; Power Conversion Efficiency.

I. INTRODUCTION

The global transition from fossil fuels to renewable energy is driven by increasing energy demand, population growth, and environmental concerns. Addressing these challenges requires the development of cost-effective energy technologies based on locally available and sustainable materials [1]. Photovoltaic (PV) systems convert sunlight directly into electrical energy through the photovoltaic effect and have become a central component of global renewable energy strategies [2]. Over the past decades, PV technologies have undergone significant advancements in materials, device architectures, and fabrication techniques aimed at improving efficiency and scalability [3]. Among these technologies, dye-sensitized solar cells (DSSCs) have emerged as a promising alternative because of their low production cost, simple fabrication processes, and unique operational mechanism. First introduced by O'Regan and Grätzel [4], DSSCs separate the functions of light absorption and charge transport, where a sensitizing dye adsorbed on a wide-bandgap semiconductor such as titanium dioxide (TiO₂) absorbs photons and injects electrons into the semiconductor conduction band, thereby generating electrical current.

Natural dyes have attracted considerable attention as environmentally friendly sensitizers for DSSCs. Red sorghum (*Sorghum bicolor*), a widely cultivated cereal crop, contains anthocyanin pigments that exhibit strong absorption within the visible region of the solar spectrum, thereby enhancing light harvesting and broadening the spectral response of DSSCs. Furthermore, red sorghum is biodegradable, inexpensive, locally available, and can be processed through relatively simple extraction procedures, making it an attractive candidate for sustainable photovoltaic applications. Its chemical structure contains functional groups capable of strong adsorption onto TiO₂ surfaces, thereby facilitating efficient electron injection and charge transfer processes [5].

DSSCs offer several advantages over conventional silicon-based solar cells. They employ inexpensive materials, require less energy-intensive fabrication methods, and can be fabricated on flexible substrates for portable, wearable, and irregular-surface applications [6]. In addition, DSSCs exhibit relatively good performance under low-light and diffuse illumination conditions, where conventional silicon solar cells often experience reduced efficiency [7].

Despite these advantages, the widespread adoption of DSSCs remains limited by challenges associated with long-term stability and environmental durability. Exposure to moisture, ultraviolet radiation, and temperature fluctuations can degrade key components such as dyes, electrolytes, and electrodes, resulting in reduced performance and shortened device lifespan [2], [8–9]. Consequently, current research efforts focus on developing durable sensitizers, stable electrolytes, and improved electrode materials capable of enhancing device efficiency and operational stability [10].

Gum Arabic, a natural polysaccharide exudate obtained from *Acacia* species, has attracted increasing attention as an

environmentally friendly biopolymer for energy-related applications. It consists primarily of high-molecular-weight polysaccharides and their calcium, magnesium, and potassium salts. The abundance of hydroxyl and carboxyl functional groups within its structure enables strong interactions with metal oxide surfaces and promotes effective film formation [11]. In DSSCs, gum Arabic can function both as a structural binder and an interfacial modifier within TiO₂ photoanodes [12]. During thermal treatment, partial decomposition of gum Arabic may generate micro- and mesoporous structures within the TiO₂ matrix, thereby increasing the available surface area for dye adsorption [13]. Enhanced porosity facilitates higher dye loading, while improved nanoparticle connectivity promotes efficient electron transport, reduced grain-boundary resistance, and improved photovoltaic performance [14].

The fabrication of DSSCs involves the integration of photoanodes, sensitizing dyes, electrolytes, and counter electrodes. Various deposition techniques, including screen printing, spray pyrolysis, and doctor-blading, have been employed to prepare TiO₂ photoanodes. Among these methods, the doctor-blade technique offers precise control of film thickness, substrate versatility, simplicity, and scalability for large-area device fabrication [15].

Despite significant advances in DSSC technology, achieving an optimal balance between efficiency, stability, and cost remains a major challenge, particularly in devices utilizing natural dye sensitizers. Although TiO₂ photoanodes and anthocyanin-rich dyes such as red sorghum have demonstrated promising light-harvesting capabilities, poor long-term stability, weak interfacial bonding, and inefficient charge transport continue to limit device performance. Furthermore, limited attention has been given to the use of indigenous biopolymers for improving photoanode architecture and interfacial charge-transfer processes.

Therefore, this study investigates the role of gum Arabic as a natural biopolymeric binder and interfacial modifier in TiO₂-based DSSCs sensitized with red sorghum dye. Particular emphasis is placed on evaluating its influence on film morphology, dye adsorption, charge transport, and photovoltaic performance. The study aims to contribute to the development of low-cost, sustainable, and locally sourced DSSCs with enhanced efficiency and operational stability.

II. MATERIALS AND METHODS

A. Materials

Titanium (IV) isopropoxide (TIP, ≥97%, Sigma-Aldrich) was employed as the titanium precursor for TiO₂ synthesis. Citric acid monohydrate (Molychem) functioned as both a complexing agent and combustion fuel, while ammonium nitrate (NH₄NO₃, Molychem) served as the oxidizing agent. Concentrated nitric acid (Guangdong Chemicals) was utilized to stabilize the titanium precursor during the hydrolysis process. Distilled water was used as the solvent throughout the experiments without additional purification. Indium tin oxide (ITO)-coated glass substrates were used as transparent

conductive electrodes. Additional materials included a digital weighing balance, micrometer screw gauge, digital multimeter, gum Arabic, and red sorghum grains. All reagents were of analytical grade and used as received without further modification.

B. Methods

1) Preparation of TiO₂ Ink with Gum Arabic Binder

Gum acacia was sourced locally from Damaturu Local Government Area, Yobe State, Nigeria, and pulverized using a mechanical blender. TiO₂ inks were formulated with 5 g of nanocrystalline TiO₂ powder per batch. Two concentrations of gum Arabic were evaluated: Sample A (0.56 g in 6 mL warm distilled water, ~50 °C) and Sample B (1.25 g in 6 mL warm distilled water under identical conditions). Each was stirred magnetically until a homogeneous, viscous solution was formed. TiO₂ powder was gradually incorporated into the binder solution with continuous grinding in a ceramic mortar for 1 h to prevent agglomeration. Ink viscosity was adjusted by either adding distilled water or allowing controlled evaporation, optimizing consistency for the doctor-blade deposition method.

2) Preparation of Sorghum Dye Extract

Red sorghum (*Sorghum bicolor*) grains were sourced locally from Potiskum Local Government Area, Yobe State, Nigeria. The dried grains were mechanically ground into fine powder. Approximately 20 g of the powdered sample was soaked in a solvent mixture of ethanol and methanol in a 2:1 volumetric ratio for 12 hours to facilitate pigment extraction. The mixture was subsequently filtered to remove solid residues, and the filtrate was centrifuged to eliminate remaining particulates. The resulting dye extract was used directly in the fabrication of dye-sensitized solar cells (DSSCs) at ambient temperature.

3) Fabrication of Dye-Sensitized Solar Cells

Photoanodes were prepared via the doctor-blade method. ITO-coated glass substrates were sequentially cleaned with isopropanol, ethanol, and deionized water, then air-dried. Sellotape spacers defined the film thickness and uncoated regions for electrical contacts. Carbon paste (Elcocarb, Solaronix) was applied as the counter electrode by doctor-blading and annealed at 400 °C for 30 min. Mesoporous TiO₂ films from Sample A and Sample B were deposited by the blade method and sintered at 450 °C for 30 min to ensure particle connectivity and substrate adhesion. Film thickness was about 0.009 mm ($d = 9 \mu\text{m}$) with an active area of $(0.4 \times 0.8) \text{ cm}^2$. Dye adsorption involved immersing the mesoporous films in the red sorghum extract overnight, followed by rinsing with methanol and drying at 60 °C for 30 min in darkness. The conductive side of the transparent electrodes was gently placed on top of the conducting, carbonized side of the counter electrodes, with parafilm serving as a spacer. The assembled cells incorporated a 0.5 mL iodide/triiodide electrolyte (iodine electrolyte solution) between the photoanode and carbon counter electrode. The binder clips attached to the glass slides were cleaned with ethanol before being placed on the dyed

working electrodes, with electrical contacts established via silver paste on uncoated electrode regions.

4) Characterization Techniques

Structural, optical, and PV electrical analyses were conducted to evaluate the physicochemical properties of the dye extract and photoelectrodes. Ultraviolet-Visible (UV-VIS) spectroscopy (UV-750 Series) was employed to investigate the optical characteristics of the sorghum dye. Fourier-transform infrared (FTIR) spectroscopy (Agilent MicroLab) was used to identify functional groups and assess potential interactions between the dye molecules and the TiO₂ surface, and was interpreted based on standard infrared band assignments. Photovoltaic performance of the fabricated DSSCs was evaluated by measuring key device parameters, including open-circuit voltage (V_{oc}), short-circuit current density (J_{sc}), fill factor (FF), and power conversion efficiency (PCE). Current-voltage (J-V) characteristics were recorded using a calibrated AM 1.5 solar simulator (Newport Oriel Instruments, Model 69922) with an illumination intensity of 1000 W/m². Electrical measurements were performed using a computer-controlled digital source meter (Keithley, Model 2400). The experiments were conducted at the Sheda Science and Technology Complex, Abuja, Nigeria.

III. RESULTS AND DISCUSSION

Fourier Transform Infrared (FTIR) spectroscopy was used to characterize the chemical functional groups present in the red sorghum extract and gum Arabic samples. The observed absorption bands correspond to different molecular vibrational modes, allowing for the identification of functional groups that contribute to the chemical composition of the samples.

The FTIR spectrum of the red sorghum (*Sorghum bicolor*) extract is presented in Fig. 1, while the corresponding spectral peaks are summarized in Table I. The detected peaks indicated the presence of multiple organic functional groups typical of plant-derived biomolecules.

For the red sorghum extract shown in Fig. 1, the presence of a broad absorption band around 3200-3300 cm⁻¹ corresponds to O-H stretching vibrations associated with hydroxyl groups typically found in polyphenols, flavonoids, and anthocyanin pigments [16]. These hydroxyl groups are critical in DSSC applications because they serve as anchoring sites for adsorption onto the TiO₂ semiconductor surface, facilitating the formation of stable dye-semiconductor complexes.

Table I. Spectral Peak Analysis for Red Sorghum.

Peak Number	Wavenumber (cm ⁻¹)	Intensity
1	1013.84	54.31
2	1110.75	91.74
3	1416.39	91.04
4	1647.48	79.56
5	2117.13	97.62
6	2840.23	93.19
7	3265.15	55.06

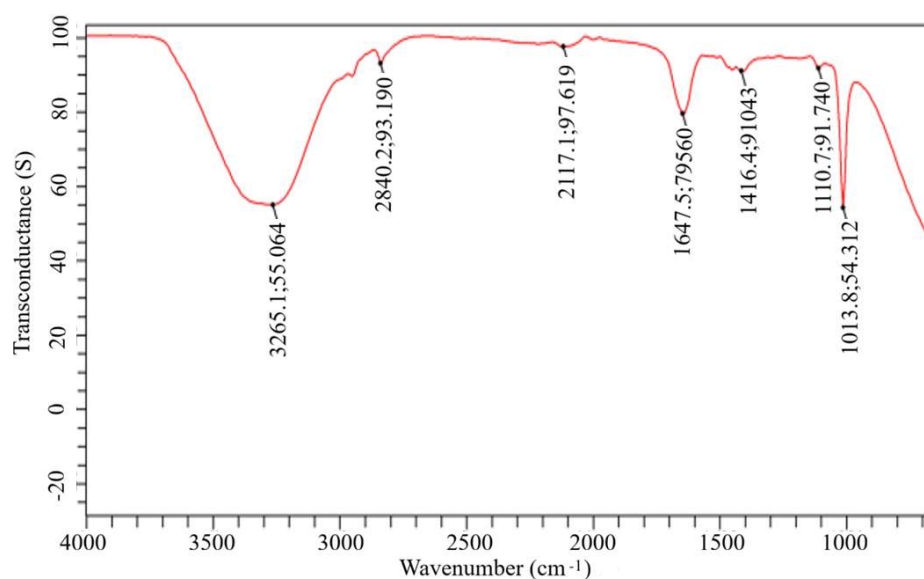


Fig. 1. FTIR spectroscopy results for the Red Sorghum sample.

Also, strong chemical attachment improves electronic coupling between the dye molecules and the conduction band of TiO_2 , thereby enhancing electron injection efficiency and reducing dye desorption during device operation [17]. The $\text{C}\equiv\text{C}$ triple-bond absorption observed at approximately 2117 cm^{-1} may indicate the presence of alkynes or nitriles, and this band is usually medium to weak in intensity [16], [18].

In addition, the FTIR band observed near 1647 cm^{-1} in the red sorghum extract corresponded to aromatic $\text{C}=\text{C}$ stretching, indicating the presence of conjugated aromatic structures [16]. Conjugated systems are particularly advantageous for DSSCs because they promote extended π -electron delocalization, which enhances light absorption in the visible region and facilitates efficient photo-induced electron transfer processes. The presence of these conjugated phenolic compounds therefore suggested that red sorghum extract can function effectively as a natural photosensitizer capable of harvesting solar radiation and generating excited electrons for injection into the semiconductor conduction band.

Furthermore, the peaks observed within the $1000\text{--}1100\text{ cm}^{-1}$ region, attributed to $\text{C}-\text{O}$ and $\text{C}-\text{C}$ stretching vibrations, indicated the presence of glycosidic linkages and oxygen-containing functional groups in the extract [19]. Such functional groups could further contribute to improved binding affinity to oxide surfaces, thereby enhancing dye loading on TiO_2 nanoparticles. Higher dye loading generally increases the number of photoactive molecules available for light absorption, which can improve the short-circuit current density (J_{sc}) of DSSCs.

The FTIR spectral peaks of gum Arabic are summarized in Table II, and the corresponding FTIR spectrum is presented in Fig. 2. The identified absorption bands reveal the presence of characteristic functional groups typical of polysaccharide-based biomaterials.

The FTIR spectrum of gum Arabic in Fig. 2 may contribute to revealing complementary structural characteristics that support its role as a stabilizing and functional component in DSSC systems. The broad $\text{O}-\text{H}$ stretching band near $3265\text{--}3400\text{ cm}^{-1}$ indicated the presence of abundant hydroxyl groups typical of polysaccharide biopolymers. These hydroxyl groups contributed to hydrogen bonding interactions and film-forming capability, which can enhance the structural integrity of the photoanode layer or electrolyte matrix [20-21]. Such properties may be beneficial for maintaining mechanical stability and improving the durability of DSSC devices during prolonged operation.

A significant spectral feature in gum Arabic is the carbonyl ($\text{C}=\text{O}$) absorption band around 1729 cm^{-1} , which suggests the presence of ester or carboxylic acid functionalities associated with uronic acid residues in the polysaccharide structure. These functional groups are known to facilitate coordination interactions with metal oxide surfaces, potentially improving the adhesion of organic dyes to TiO_2 and promoting efficient interfacial charge transfer. Additionally, carboxylate groups enhance ionic mobility within the electrolyte environment, thereby improving charge transport and reducing recombination losses within the DSSC system [20-21].

Table II. Spectral Peak Analysis for the Gum Arabic.

Peak Number	Wavenumber (cm^{-1})	Intensity
1	976.56	76.00
2	1237.48	90.34
3	1371.66	92.26
4	1602.76	92.16
5	1729.48	95.08
6	2884.96	96.31
7	3265.15	92.20

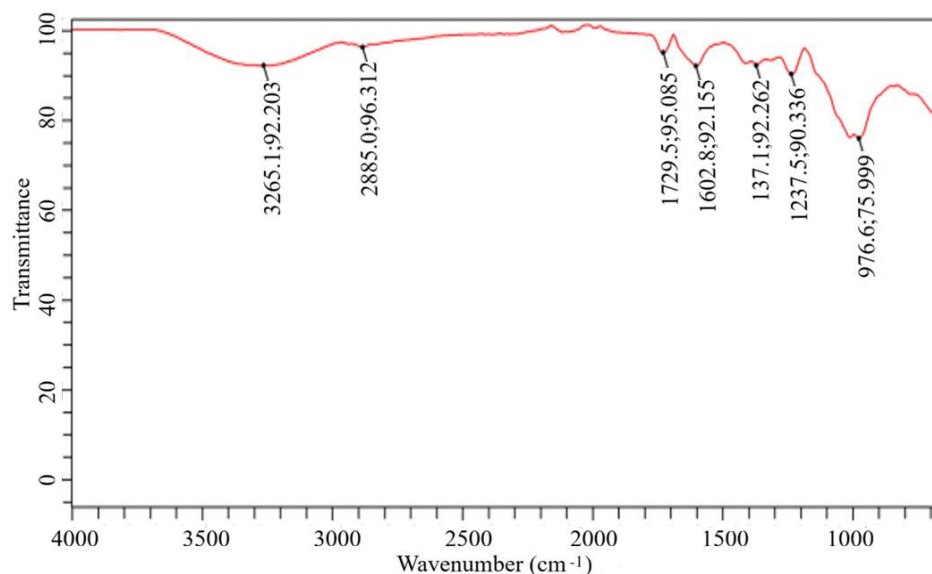


Fig. 2. FTIR spectroscopy results for the gum Arabic.

Fig. 3 presents the comparative FTIR spectra of red sorghum extract and gum Arabic, while Tables III and IV summarize the quantitative comparison of their major absorption peaks. The analysis revealed the presence of common hydroxyl and oxygen-containing functional groups in both materials, indicating their potential compatibility in dye-sensitized solar cell (DSSC) applications. However, distinct spectral characteristics suggest different functional roles. The red sorghum extract exhibited absorption bands associated with phenolic compounds and conjugated molecular structures, which are favorable for light harvesting and photo-induced electron generation [22–23]. In contrast, gum Arabic showed features characteristic of polysaccharide-based materials, supporting its role in enhancing structural integrity, interfacial adhesion, and ionic transport within the DSSC architecture. These complementary properties may contribute to improved photovoltaic performance and device stability.

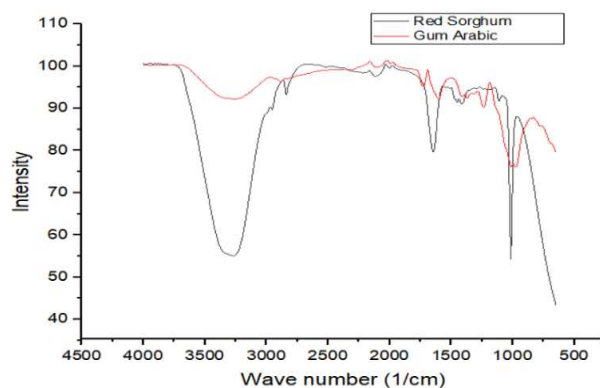


Fig. 3. FTIR spectroscopy results for the grains of red sorghum and gum Arabic.

Table III. Comparison of FTIR Peaks (Technical Analysis).

Peak No.	Red Sorghum, Wavenumber (cm ⁻¹)	Red Sorghum, Intensity	Gum Arabic, Wavenumber (cm ⁻¹)	Gum Arabic, Intensity
1	1013.84	54.31	976.56	76.00
2	1110.75	91.74	1237.48	90.34
3	1416.39	91.04	1371.66	92.26
4	1647.48	79.56	1602.76	92.16
5	2117.13	97.62	1729.48	95.08
6	2840.23	93.19	2884.96	96.31
7	3265.15	55.06	3265.15	92.20

Table IV. Comparison Overview.

Feature	Red Sorghum Sample	Gum Arabic Sample
C=O (carbonyl) peak (~1729 cm ⁻¹)	Absent	Present
Triple bond (~2117 cm ⁻¹)	Present	Absent
C–O or C–O–C peaks (1000–1200 cm ⁻¹)	1014, 1111 cm ⁻¹	976, 1237 cm ⁻¹
CH ₂ bending (~1415 cm ⁻¹)	1416 cm ⁻¹	1372 cm ⁻¹
Amide/C=C (~1600–1650 cm ⁻¹)	1647 cm ⁻¹	1603 cm ⁻¹
O–H/N–H stretching (~3200–3300 cm ⁻¹)	3265 cm ⁻¹ (moderate)	3265 cm ⁻¹ (strong)
C–H stretching (~2850–2950 cm ⁻¹)	2840 cm ⁻¹	2885 cm ⁻¹

The coexistence of these complementary functional groups suggested a synergistic interaction between the natural dye and the biopolymeric matrix [20–21]. Hydroxyl and carboxylate functionalities may be attributed to promoting effective dye adsorption and electron injection, while the polysaccharide framework of gum Arabic is likely associated with enhancing film formation and charge transport pathways.

Such synergistic effects may contribute to improved photocurrent generation, reduced recombination losses, and enhanced stability of DSSCs fabricated using red sorghum dye and gum Arabic components [20], [21].

The coexistence of these complementary functional groups suggested a synergistic interaction between the natural dye and the biopolymeric matrix [20-21]. Hydroxyl and carboxylate functionalities may be attributed to promoting effective dye adsorption and electron injection, while the polysaccharide framework of gum Arabic is likely associated with enhancing film formation and charge transport pathways. Such synergistic effects may contribute to improved photocurrent generation, reduced recombination losses, and enhanced stability of DSSCs fabricated using red sorghum dye and gum Arabic components [20-21].

Overall, the FTIR findings confirmed that the chemical functionalities present in red sorghum extract and gum Arabic are well-suited for DSSC applications. The presence of anchoring groups ($-OH$, $-COOH$), conjugated aromatic structures, and polysaccharide networks may be attributed to collectively supporting efficient light harvesting, electron transfer, and structural stabilization within the device architecture. These characteristics highlighted the potential of combining natural plant dyes and biopolymer materials as sustainable and low-cost alternatives for the development of environmentally friendly dye-sensitized solar cells [17].

Fig. 4 presents the UV-Vis absorbance spectrum of untreated TiO_2 -coated glass. The untreated TiO_2 film exhibited absorption predominantly in the ultraviolet region, reflecting its wide band gap (~ 3.2 eV), and confirmed that pristine TiO_2 is largely inactive under visible-light irradiation.

The spectrum in Fig. 4 showed strong ultraviolet absorption below approximately 400 nm with a distinct absorption edge near the UV-visible boundary. Minimal absorption occurred across the visible and near-infrared regions, indicating the wide band-gap nature of anatase TiO_2 and confirming that the untreated film primarily interacts with ultraviolet radiation.

In conventional TiO_2 photoanodes, the wide band gap (~ 3.2 eV) restricted photon absorption primarily to the ultraviolet region, which represented only a small fraction of the solar spectrum. Consequently, untreated TiO_2 films contributed minimally to solar energy conversion under visible-light illumination.

Fig. 5 presents the UV-Vis absorbance spectrum of TiO_2 -coated glass after immersion in distilled water. The optical absorbance spectrum of the TiO_2 -coated glass following immersion in distilled water exhibits markedly different spectral behavior compared with the untreated film.

The spectrum in Fig. 5 revealed pronounced absorption across the visible region (500-600 nm), followed by a gradual decrease toward the near-infrared range. The shift in the absorption edge suggested the formation of defect-related states or structural modifications that extended the optical response of TiO_2 into the visible region.

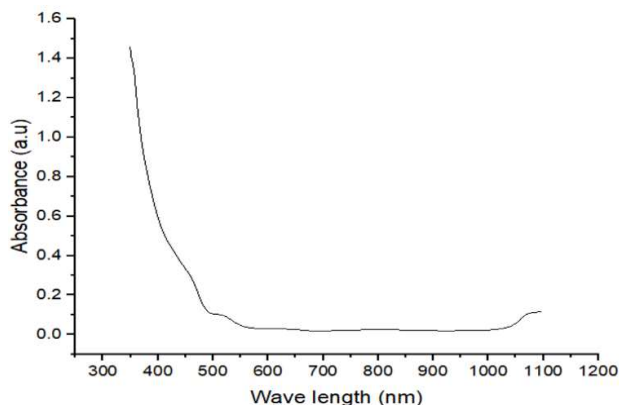


Fig. 4. UV-Vis absorbance spectrum of untreated TiO_2 -coated glass showing strong ultraviolet absorption and minimal visible light interaction.

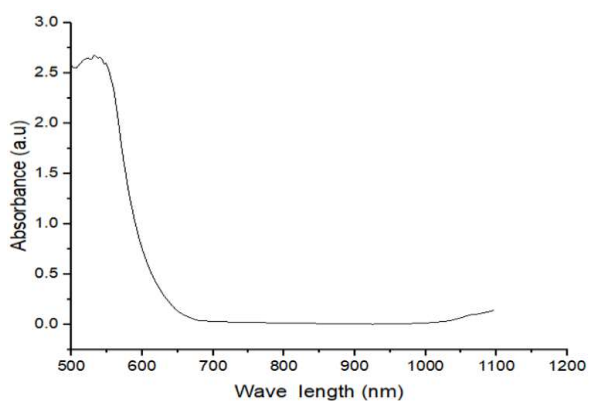


Fig. 5. UV-Vis absorbance spectrum of TiO_2 -coated glass after immersion in distilled water showing extended visible-light absorption and a red-shifted absorption edge.

Furthermore, the defect states observed in the water-treated TiO_2 film may also contribute to enhancing visible-light absorption by introducing intermediate energy levels within the band structure. However, excessive defect formation may act as recombination centers that reduce charge transport efficiency. These imperfections created additional energy states, which allowed the film to absorb longer wavelengths than expected. Using the absorption edge around 643 nm, the band gap was estimated to be approximately 1.9 eV, which is lower than the standard ~ 3.2 eV for anatase TiO_2 .

Fig. 6 presents the UV-Vis absorbance spectrum of TiO_2 -coated glass sensitized with red sorghum extract. This spectral behavior indicated the sensitized film effectively absorbs high-energy visible photons while transmitting longer wavelengths.

In Fig. 6, enhanced absorption was observed in the near-UV and visible regions due to the adsorption of anthocyanin-rich chromophores from the red sorghum extract. The broadened spectral response indicated effective dye loading and demonstrates the potential of red sorghum as a natural sensitizer for dye-sensitized solar cells. Upon photoexcitation,

these dye molecules injected electrons into the conduction band of TiO_2 , enabling charge transport through the semiconductor network.

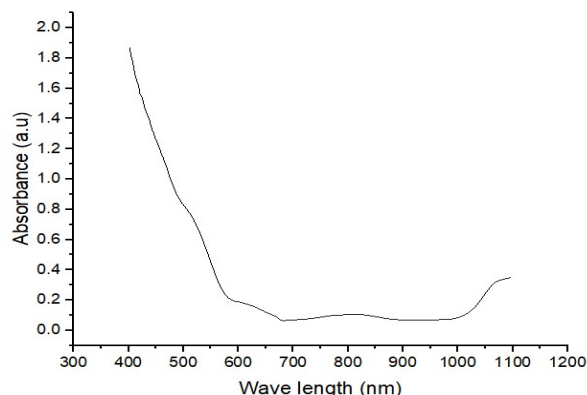


Fig. 6. UV-Vis absorbance spectrum of TiO_2 -coated glass sensitized with red sorghum extract showing enhanced absorption in the visible region due to anthocyanin dye adsorption.

Dye sensitization offers a more controlled mechanism for extending light absorption while preserving the intrinsic electron transport properties of TiO_2 . These findings highlighted the importance of sensitizer selection and surface engineering strategies in optimizing DSSC photoanodes for improved photovoltaic performance [4], [24].

Fig. 7 presents the comparative UV-Vis absorbance spectra of untreated TiO_2 , water-treated TiO_2 , and red sorghum-sensitized TiO_2 films. A comparative analysis of the three spectra provided important insight into how environmental treatment and dye sensitization influence the optical behavior of TiO_2 thin films.

In Fig. 7, the comparative spectra illustrated the significant influence of environmental treatment and dye adsorption on the optical behavior of TiO_2 thin films. While untreated TiO_2 absorbed predominantly in the ultraviolet region, both water treatment and dye sensitization extend absorption into the visible region, enhancing the light-harvesting capability of the material.

Overall, the UV-Vis analysis demonstrated that both environmental treatment and natural dye sensitization significantly modified the optical behavior of TiO_2 thin films. While pristine TiO_2 exhibited strong ultraviolet absorption due to its wide band gap, the introduction of defect states or dye molecules extended the spectral response into the visible region. Among the investigated samples, the red sorghum-sensitized TiO_2 film showed the most promising light-harvesting characteristics for DSSC applications due to its enhanced visible absorption and effective dye semiconductor interaction. These results supported the potential use of natural sorghum-derived dyes as sustainable and low-cost sensitizers for next-generation photovoltaic devices.

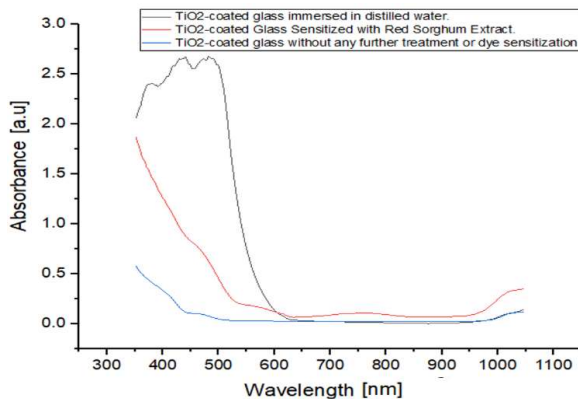


Fig. 7. Comparative UV-Vis absorbance spectra of untreated TiO_2 , water-treated TiO_2 , and red sorghum-sensitized TiO_2 films showing the extension of light absorption into the visible region.

The photovoltaic performance of the fabricated DSSC samples was evaluated through current-voltage (J-V) characterization under dark and illuminated conditions. The J-V curves presented in Fig. 8-11 provided quantitative information on the photoelectrochemical behavior of the devices. Key photovoltaic parameters, including open-circuit voltage (V_{oc}), short-circuit current density (J_{sc}), maximum power output (P_{max}), fill factor (FF), and power conversion efficiency (η), were calculated using standard photovoltaic relationships [4], [25].

Fig. 8 presents the J-V characteristics of Sample A under dark conditions. The curve under these conditions reflected higher internal resistance and limited charge carrier generation.

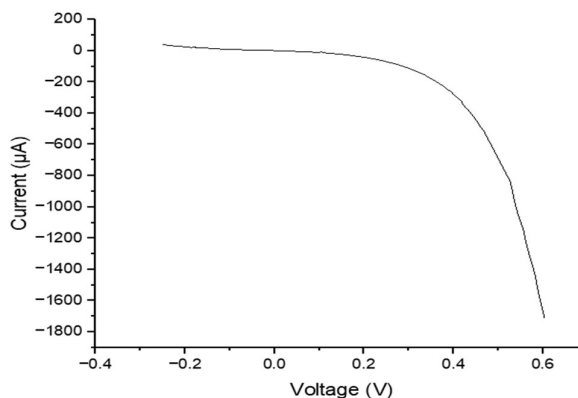


Fig. 8. Sample A-dark.

The J-V characteristics of the sample A DSSC measured under dark conditions are presented in Fig. 8. The device exhibited an open-circuit voltage of 0.30 V and a short-circuit current density of 0.50 mA/cm². The maximum power point occurred at $V_{max} = 0.20$ V and $I_{max} = 0.35$ mA/cm², producing a maximum power output of 7.0×10^{-5} mW/cm². The calculated fill factor was 0.47, resulting in a power conversion

efficiency of 0.07%. The relatively low photocurrent and rapid decline in the J-V curve indicated limited charge generation and increased recombination losses in the absence of illumination. Under dark conditions, the lack of photoexcitation suppressed electron injection from the dye molecules into the TiO₂ conduction band, leading to minimal current generation and higher internal resistance within the device [26].

Fig. 9 presents the J-V characteristics of Sample A under illumination conditions. When illuminated, the photovoltaic performance improved significantly.

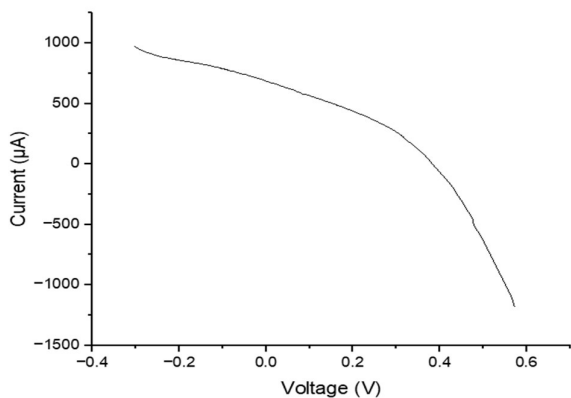


Fig. 9. Sample A-light.

Under illumination (Fig. 9), the sample A DSSC demonstrated improved photovoltaic behavior. The open-circuit voltage increased to 0.50 V while the short-circuit current density rose to 0.90 mA/cm². The maximum power output occurred at $V_{\max} = 0.38$ V and $I_{\max} = 0.70$ mA/cm², yielding $P_{\max} = 2.7 \times 10^{-4}$ mW/cm². The fill factor increased to 0.59, resulting in a conversion efficiency of 0.27%. The enhanced device response under illumination confirmed the effective sensitization of TiO₂ by the red sorghum dye. Photoexcitation of anthocyanin molecules within the dye extract promoted electron injection into the TiO₂ conduction band, generating photocurrent through the external circuit. Similar behavior has been reported for DSSCs sensitized with natural pigments such as hibiscus and berry extracts [24].

Fig. 10 presents the J-V characteristics of Sample B under dark conditions. The improved performance suggested that higher gum Arabic content may enhance film morphology and charge transport properties within the TiO₂ photoanode.

The J-V characteristics of Sample B DSSC measured under dark conditions are presented in Fig. 10. The device recorded an open-circuit voltage of 0.55 V and a short-circuit current density of 1.20 mA/cm². The maximum power output occurred at $V_{\max} = 0.42$ V and $I_{\max} = 0.95$ mA/cm², corresponding to $P_{\max} = 4.0 \times 10^{-4}$ mW/cm². The fill factor increased to 0.61, and the calculated efficiency reached 40%. Compared with the 10 % gum Arabic device, the improved performance indicated that increasing gum Arabic

concentration could enhance the structural properties of the TiO₂ film. The natural polymer is likely associated with improved particle binding and film uniformity, possibly due to improved electron transport pathways, and may contribute to reduced recombination losses at the semiconductor-electrolyte interface [25].

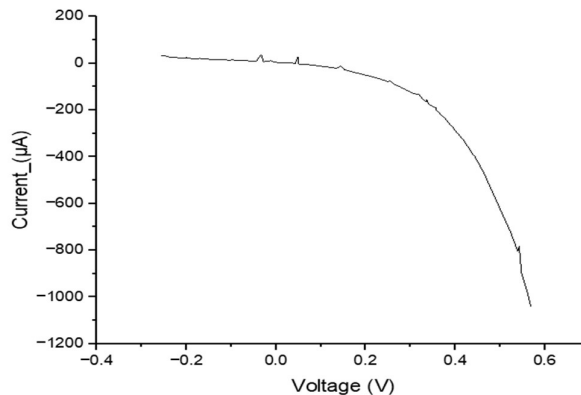


Fig. 10. Sample B-dark.

Fig. 11 presents the J-V characteristics of Sample B under light conditions. The improvement in device efficiency can be attributed to enhanced dye adsorption, improved TiO₂ film connectivity, and more efficient electron transport within the photoanode.

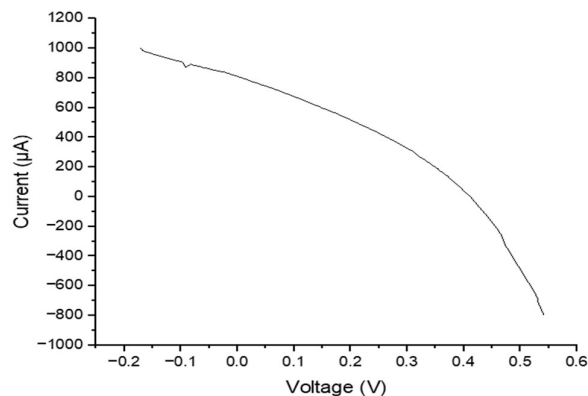


Fig. 11. Sample B, light.

The best photovoltaic performance was observed for the sample B DSSC under illumination (Fig. 11). The device exhibited an open-circuit voltage of 0.60 V and a short-circuit current density of 1.50 mA/cm². The optimal operating point occurred at $V_{\max} = 0.46$ V and $I_{\max} = 1.15$ mA/cm², producing a maximum power output of 5.3×10^{-4} mW/cm². Although the fill factor was moderate (0.59), the device achieved the highest power conversion efficiency of 53%. This improvement indicated that a higher gum Arabic concentration is likely to enhance the TiO₂ film connectivity and increase the available surface area for dye adsorption. Improved dye loading promotes stronger light harvesting and more efficient electron

injection into the TiO₂ conduction band, resulting in enhanced photocurrent generation.

A. Influence of Illumination and Internal Resistance

The slope of the J-V curves provided insight into the internal resistance and charge transport characteristics of the DSSC devices. Under dark conditions (Figs. 8 and 10), the curves exhibited steeper slopes due to minimal charge carrier generation, indicating higher internal resistance. In contrast, under illuminated conditions (Figs. 9 and 11), the slopes become less steep as photocurrent increases, reflecting improved charge mobility and reduced effective resistance within the device. This behavior confirmed the fundamental operating mechanism of DSSCs, where photoexcited dye molecules injected electrons into the TiO₂ conduction band and the resulting electrons migrated through the semiconductor network toward the external circuit [4], [25].

B. Role of Gum Arabic in the DSSC Performance

At the dye-semiconductor interface, gum Arabic enhances adsorption stability and electronic coupling between the dye molecules and TiO₂ surface through hydrogen bonding and electrostatic interactions. This stabilization reduces dye desorption and improves electron injection efficiency from the excited dye into the TiO₂ conduction band. Furthermore, gum Arabic introduces a thin insulating organic layer that suppresses charge recombination by limiting direct contact between injected electrons and the redox electrolyte (I⁻/I₃⁻). This recombination barrier increases electron lifetime and elevates open-circuit voltage (V_{oc}). However, due to its inherently insulating nature, excessive incorporation may hinder electron mobility and increase internal resistance, highlighting the need for optimal concentration. Its hydrophilic character also enhances electrolyte wettability and penetration into the porous network, ensuring efficient dye regeneration and continuous redox cycling, which are critical for maintaining steady-state device performance.

Thermally controlled decomposition of gum Arabic may leave behind beneficial carbonaceous residues that improve inter-particle electrical connectivity, although incomplete removal can introduce trap states and resistive losses. Experimentally, incorporation of gum Arabic or similar biopolymers has been shown to improve DSSC performance parameters, with typical increases in J_{sc}, V_{oc}, and FF leading to overall efficiency enhancements, particularly in natural dye-based systems. In applications such as red sorghum (anthocyanin) DSSCs, gum Arabic is especially valuable for improving dye retention, stability under illumination, and interfacial durability. Overall, its integration provides a sustainable, low-cost, and environmentally friendly alternative to synthetic binders, while simultaneously enhancing the structural, optical, and electrochemical properties of DSSCs when carefully optimized.

Therefore, the incorporation of gum Arabic as a polymeric binder within the TiO₂ photoanode significantly improves device performance. Increasing the gum Arabic concentration from Sample A to Sample B is likely associated with enhanced film adhesion, improved nanoparticle connectivity, and increased surface area available for dye adsorption. These structural improvements facilitated more efficient electron transport through the TiO₂ network while simultaneously suppressing charge recombination at the semiconductor-electrolyte interface. Consequently, the photocurrent density increases, and the overall photovoltaic response improves under illumination. The results demonstrate that gum Arabic can serve as an effective natural binder for improving the structural and electrochemical properties of TiO₂ photoanodes in DSSCs.

C. PV Electrical Analysis

DSSC performance is quantified using four key parameters: open-circuit voltage (V_{oc}), short-circuit current density (J_{sc}), fill factor (FF), and power conversion efficiency (η). These are derived from current density-voltage (J-V) characteristics. The fill factor represents the ratio of maximum extractable power to the product of V_{oc} and J_{sc}, indicating the “squareness” of the J-V curve [27]. The overall efficiency is expressed as:

$$FF = \frac{P_{\max}}{J_{sc} V_{oc}} = \frac{V_{\max} I_{\max}}{J_{sc} V_{oc}} \quad (1)$$

The electrical power conversion efficiency of a solar cell is determined by the ratio of the power output to the power input. The efficiency of a solar cell can be determined from its J-V characteristic curve as follows:

$$\eta = \frac{P_{\max}}{P_{in}} \times 100 \% \quad (2)$$

$$\text{But, } P_{\max} = FF \times J_{sc} V_{oc} \quad (3)$$

$$\therefore \eta = \left(\frac{FF \times J_{sc} V_{oc}}{P_{in}} \right) \times 100 \% = \left(\frac{P_{\max}}{P_{in}} \right) \times 100 \% \quad (4)$$

From Fig. 11, the short circuit current density and open circuit voltage obtained directly from the Excel plot are J_{sc} = 1.50 mA/cm², and V_{oc} = 0.60 V.

The maximum output power density obtained from Table V is P_{max output} = 5.3 × 10⁻⁴ mW/cm². Also, Active area A_c = (0.4 × 0.8) cm² = 0.32 cm², illumination intensity E = 1000 W/m² = 100 mW/cm², and (Power Density)_{input} = (E × A_c) / 0.32 cm² = (100 mW/cm² × 0.32 cm²) / 0.32 cm² = 100 mW/cm².

Using (1) and (4),

$$FF = (\text{Power density})_{input} / V_{oc} \times J_{sc} = 5.3 \times 10^{-4} / (0.60 \times 1.50) \times 10^{-3} = 0.59$$

$$\eta = (\text{Power density})_{input} / (\text{Power Density})_{input} \times 100 \% = 5.3 \times 10^{-4} / 100 \times 10^{-3} = 0.53 \%$$

Therefore, using (1) and (4), the photovoltaic parameters (J_{sc}, V_{oc}, V_{max}, I_{max}, P_{max}, FF, and η) of the TiO₂/red sorghum dye-sensitized solar cells were calculated and are summarized in Table V.

Table V. Summarized Output J-V Parameters of TiO₂ - Red Sorghum Grain Bicolor Extract DSSC in Samples A and B (Combined J-V Parameters).

Samples	V _{oc} (V)	J _{sc} (mA/cm ²)	V _{max} (V)	I _{max} (mA/cm ²)	P _{max} (mW/cm ²)	FF	η (%)
Sample A-dark	0.30	0.50	0.20	0.35	0.00007		
Sample A-light	0.50	0.90	0.38	0.70	0.00027	0.59	0.27
Sample B-dark	0.55	1.20	0.42	0.95	0.00040		
Sample B-light	0.60	1.50	0.46	1.15	0.00053	0.59	0.53

This work reported an optimum value of 0.53% for power conversion efficiency, which is reasonably good when compared with the work of [28], who showed that the use of gum Arabic treated with potassium bromide in dye-sensitized solar cell architectures with various natural dyes (FTO/Gum Doping by potassium bromide/Saffron Dye/FTO+Graphene + Iodine, FTO/Gum Doping by potassium bromide/Henna Dye/FTO+Graphene + Iodine, and FTO/Gum Doping by potassium bromide/Blue 8GX dyes / Dye/ FTO+Graphene + Iodine) gave decent photovoltaic performance (4.91 mA/cm², 0.25 V, 0.099%, 0.80; 4.31 mA/cm², 1.457 V, 0.76, 0.46%; and 7.45 mA/cm², 1.199 V, 0.68, 0.56%, respectively). From the result obtained, it can be inferred that gum Arabic has remarkable electrical properties, and because it is affordable and relatively easy to prepare, it inspires cost-effective design of solid-state dye-sensitized solar cells.

In a related investigation, [29] developed gum Arabic-based DSSCs using several sensitizing dyes, namely EnChroma Black, Coumarin 500, DDTc, Nile Blue, and Rhodamine B, in a device arrangement consisting of ITO/gum Arabic/dye/ITO + graphite/iodine. The corresponding power conversion efficiencies recorded were 1.9, 4.92, 0.44, 0.37, and 2.01%, respectively. Among all the dyes examined, Coumarin 500 produced the highest efficiency, which was linked to its favorable optical transparency and enhanced capability for visible-light harvesting. The improved transparency likely promoted greater photon penetration into the active layer, thereby facilitating more effective exciton generation and charge separation within the gum Arabic-based system. The results further emphasized the importance of compatibility between the sensitizer and polymer matrix in determining DSSC performance.

Reference [30] also reported a gum Arabic + CuO dye photoactive system, which showed a relatively low efficiency of 0.37%; it exhibited a remarkably high fill factor of 0.98, indicating efficient charge extraction and reduced internal resistance within the device. The low overall efficiency was primarily attributed to its very small open-circuit voltage (0.0157 V), insufficient light absorption, and limited transparency of the gum Arabic layer. Previous reports also suggest that the arrangement of the DSSC layers strongly affects the performance of gum Arabic-containing devices; placing a more transparent gum Arabic layer above the dye enhances light penetration and improves photon harvesting efficiency.

IV. CONCLUSION

This study demonstrates that extract from Sorghum bicolor is a viable natural photosensitizer for dye-sensitized solar cells (DSSCs), owing to its anthocyanin-rich composition and strong absorption in the visible region (400-600 nm). The presence of functional groups such as hydroxyl, carboxyl, and aromatic bonds enhances effective adsorption onto titanium dioxide and facilitates efficient electron transfer. The addition of gum Arabic as a binder may improve the structural integrity and uniformity of the photoanode, leading to better dye loading and interfacial stability. Photovoltaic evaluation confirmed measurable device performance, with a maximum power conversion efficiency of 0.53% under optimized conditions comparable to other natural dye systems and indicative of the promise of locally sourced biomaterials for sustainable solar energy applications.

Future work should focus on optimizing dye extraction and sensitization parameters, enhancing electrode fabrication techniques, and exploring co-sensitization and alternative bio-derived materials to improve efficiency. Additionally, studies on long-term stability and the adoption of solid-state or quasi-solid electrolytes are recommended to advance the durability, scalability, and overall performance of natural dye-based DSSCs.

ACKNOWLEDGMENT

The I-V characterization was carried out at the Sheda Science and Technology Complex (SHESTCO), Kwali, Abuja, Nigeria, while the FTIR measurements were performed at the Central Laboratory, Umaru Musa Yar'adua University, Katsina, Nigeria. The authors gratefully acknowledge the support provided by the staff of these facilities and the Department of Physics, Kaduna State University, Kaduna, Nigeria.

References

- [1] F. Akingbade, A. Boyo, S. Oluwole, and I. Abudusalami, "Assembly of dye-sensitized solar cell using the stem and grain of Sorghum bicolor as sensitizers." *J. Nat. Sci. Res.*, vol. 3, no. 5, pp. 13-24, 2013.
- [2] M. A. Green, K. Emery, Y. Hishikawa, W. Warta, and E. D. Dunlop, "Solar cell efficiency tables

- (Version 54),” *Prog. Photovolt. Res. Appl.*, vol. 27, no. 1, pp. 3–12, 2019.
- [3] A. Al-Alawi, S. Al-Saadi, L. L. Kazmerski, and T. S. Jawad, “Review of photovoltaic materials, applications, and technologies,” *Renew. Sustain. Energy Rev.*, vol. 71, pp. 735–743, 2017.
- [4] B. O’Regan and M. Grätzel, “A low-cost, high-efficiency solar cell based on dye-sensitized colloidal TiO₂ films,” *Nature*, vol. 353, pp. 737–740, 1991.
- [5] M. S. Kallo, A. M. Abdoukadi, S. B. Abdourahmane, and A. Rabani, “Dye-sensitized solar cell using natural anthocyanin dyes extracted from Sorghum spp. (Poaceae) sheaths,” *IOSR J. Appl. Chem.*, vol. 14, no. 9, pp. 1–9, 2021, doi: 10.9790/5736-14090101.
- [6] I. K. Mohammed, A. Y. Jibrin, I. Haruna, S. Taufiq, K. I. Aliyu, G. D. Sani, and M. I. Auwal, “Photoelectrode nanostructure dye-sensitized solar cell,” *Sci. World J.*, vol. 13, no. 1, pp. xx–xx, 2018.
- [7] J. Wu, Z. Lan, J. Lin, M. Huang, Y. Huang, and L. Fan, “High-efficiency dye-sensitized solar cells: Progress and future challenges,” *Energy Environ. Sci.*, vol. 7, no. 10, pp. 2934–2971, 2014.
- [8] T. K. Bechgaard, H. M. G. Madsen, S. Stojkovic, and O. Hagemann, “The effect of temperature on the performance of solid-state dye-sensitized solar cells,” *Electrochim. Acta*, vol. 263, pp. 397–403, 2018.
- [9] K. Kakiage, Y. Aoyama, T. Yano, K. Oya, J.-I. Fujisawa, and M. Hanaya, “Highly efficient dye-sensitized solar cells with collaborative sensitization by silyl-anchor and carboxy-anchor dyes,” *Chem. Commun.*, vol. 51, no. 20, pp. 4188–4191, 2015.
- [10] E. Mijangos, R. S. Sanchez, J. Albero, J. Garcia-Cañadas, G. Lozano, H. Garcia, and I. Mora-Seró, “Improving the stability of dye-sensitized solar cells in aqueous electrolytes at 80 °C by the use of long-lived radical initiators,” *Phys. Chem. Chem. Phys.*, vol. 17, no. 26, pp. 17169–17176, 2015.
- [11] M. Bilal, H. Munir, M. I. Khan, M. Khurshid, T. Rasheed, K. Rizwan, M. Franco, and H. M. N. Iqbal, “Gums-based engineered bio-nanostructures for greening the 21st-century biotechnological settings,” *Crit. Rev. Food Sci. Nutr.*, vol. 62, no. 14, pp. 3913–3929, 2022.
- [12] J. Morabiya, H. Bhatt, G. Prasad, and S. Bamaniya, “Polysaccharide derived light harvesting materials: A comprehensive review on enhancing performance,” *Int. Res. J. Multidiscip. Scope*, vol. 5, no. 1, pp. 504–515, 2024, doi: 10.47857/irjms.2024.v05i01.0261.
- [13] S. A. Mohamed, A. M. Elsherbini, H. R. Alrefaey, K. Adelrahman, A. Moustafa, N. M. Egodawaththa, K. E. Crawford, N. Nesnas, and S. A. Sabra, “Gum Arabic: A commodity with versatile formulations and applications,” *Nanomaterials*, vol. 15, no. 4, Art. no. 290, 2025, doi: 10.3390/nano15040290.
- [14] Y. R. Wang and S. Z. Luan, “Co-doping effects on the electronic and optical properties of β -Ga₂O₃: A first-principles investigation,” *Materials*, vol. 18, no. 9, Art. no. 2005, 2025, doi: 10.3390/ma18092005.
- [15] A. Abdulkadir, M. Almohaimeed, K. I. Aliyu, R. Abdalrheem, M. Isah, M. M. Aliyu, and A. Y. Tanko, “Influence of micro-texture sizes towards light absorption improvement in hybrid microtextured/nanotextured black silicon for solar cells,” *Int. J. Nanoelectron. Mater.*, vol. 17, no. 3, pp. 428–436, Aug. 2024.
- [16] J. Coates, “Interpretation of infrared spectra: A practical approach,” in *Encyclopedia of Analytical Chemistry*, R. A. Meyers, Ed., pp. 10815–10837, Chichester, U.K.: John Wiley & Sons, 2000.
- [17] O. A. Osowole and D. Akinyemi, “Extraction and FTIR characterization of Sorghum bicolor grain extract,” *IOSR J. Appl. Chem.*, vol. 14, no. 9, pp. 11–20, 2019, doi: 10.9790/5736-1409010109.
- [18] D. Aastha, “Spectroscopic methods for nanomaterials characterization,” in *Characterization of Nanomaterials*, Amsterdam, The Netherlands: Elsevier, 2017, pp. 73–104, doi: 10.1016/B978-0-323-46140-5.00004-2.
- [19] B. C. Smith, *Fundamentals of Fourier Transform Infrared Spectroscopy*, 2nd ed. Boca Raton, FL, USA: CRC Press, 2011.
- [20] A. Ali, S. Ahmed, M. Q. Hayat, M. Tahir, and M. F. Nisar, “FTIR characterization and nutritional analysis of gum Arabic,” *Foods*, vol. 9, no. 11, Art. no. 1546, 2020.
- [21] N. Thombare, A. Mahto, D. Singh, A. R. Chowdhury, and M. F. Ansari, “Comparative FTIR Characterization of Various Natural Gums: A Criterion for their identification,” *Journal of Polymers and the Environment*, pp. 1–9, 2023. doi: 10.1007/s10924-023-02821-1.
- [22] A. A. Moh, B. S. Wahyudi, H. Muslikhin, Y. S. Devi, and D. I. S. Fikrah, “Bioactive Compound Contents and Antioxidant Activity of Purified Red Sorghum Pericarp Extract by Membrane Ultrafiltration Process,” vol. 12, no. 1, pp. 13–19, 2023. doi: 10.22487/j24775185.2023.v12.i1.
- [23] J. C. Boulet, P. Williams and T. Doco, “A Fourier transform infrared spectroscopy study of wine polysaccharides,” *Carbohydr Polym* 69, pp. 79–85, 2007.
- [24] G. Calogero, A. Bartolotta, G. Di Marco, A. Di Carlo, and F. Bonaccorso, “Vegetable-based dye-sensitized solar cells,” *Chem. Soc. Rev.*, vol. 44, no. 10, pp. 3244–3294, 2015, doi: 10.1039/C4CS00309H.
- [25] A. Hagfeldt, G. Boschloo, L. Sun, L. Kloo, and H. Pettersson, “Dye-sensitized solar cells,” *Chem. Rev.*, vol. 110, no. 11, pp. 6595–6663, 2010.
- [26] M. Grätzel, “Dye-sensitized solar cells,” *J. Photochem. Photobiol. C Photochem. Rev.*, vol. 4, no. 2, pp. 145–153, 2003.

- [27] M. M. Isa, A. M. Nura, A. O. Musa, M. Ibrahim, and Y. A. Usman, "Numerical simulation of polycrystalline semiconductor [CdTe and Cu(In,Ga)Se₂ (CIGS)] solar cells using SCAPS 3.3.00," *Bayero J. Phys. Math. Sci.*, vol. 10, no. 1, pp. 258–266, 2019.
- [28] A. Safwa, S. Abdelsakhi, A. Yousif, E. Abdelrahman, M. H. Khalid, and E. H. Babacar, "Thin film gum Arabic doping by potassium bromide solar cells," *J. Thin Films Coat. Sci. Technol. Appl.*, vol. 7, no. 2, pp. 23–29, 2020.
- [29] D. M. Abd-Alla, A. A. A. Mohammed, I. Elkareem, M. H. Ahmed, A. A. S. Rawia, and A. Elgani, "The effect of optical energy gaps on the efficiency of dye-sensitized solar cells using gum Arabic doped by CuO and (Coumarin 500, Eriochrome Black, Rhodamine B, and DDTc) dyes," *Int. J. Innov. Sci. Eng. Technol.*, vol. 6, no. 12, pp. 38–46, 2019.
- [30] A. K. A. E. Alobid, D. A. Mubarak, I. A. Mohammed, S. M. H. Abdalsakhi, and R. A. Elgani, "The effect of transparency and replacing gum by dye layer on solar cell efficiency when doped by cobalt oxide," *Int. J. Innov. Sci. Eng. Technol.*, vol. 6, no. 12, pp. 112–120, 2019.